Biomechanical Analysis of the Effect of Finger Joint Configuration on Hand Grasping Performance: Rigid vs Flexible

Yuyang Wei, Zhenmin Zou, Zhihui Qian, Lei Ren, and Guowu Wei, *Member, IEEE*

***Abstract*— Human finger joints are conventionally simplified as rigid joints in robotic hand design and biomechanical hand modelling, due to their anatomic and morphologic complexity. However, our understanding of the effect of the finger joint configuration on the resulting hand performance is still primitive. In this study, we systematically investigate the grasping performance of the hands with the conventional rigid joints and the biomechanical flexible joints based on a computational human hand model. The measured muscle electromyography (EMG) and hand kinematic data during grasping are used as inputs for the grasping simulations. The results show that the rigid joint configuration currently used in most robotic hands leads to large reductions in hand contact force, contact pressure and contact area, compared to the flexible joint configuration. The grasping quality could be reduced up to 40% and 36% by the rigid joint configuration in terms of algebraic properties of grasping matrix and finger force limit respectively. Further investigation reveals that these reductions are caused by the weak rotational stiffness of the rigid joint configuration. This study implies that robotic/prosthetic hand performance could be improved by exploiting flexible finger joint design. Hand contact parameters and grasping performance may be underestimated by the rigid joint simplification in human hand modelling.**

***Index Terms*— Finger joint configuration, finite element human hand model, grasping quality, finger dexterity.**

I. Introduction

THE finger joint is made up of cartilage surfaces that connect two adjacent bones and determine the kinematics of the fingers. The complex function and anatomical structure of the interphalangeal joint have long been recognized [1], [2], [3], [4], [5], [6], [7], [8]. Interphalangeal ligaments and joint capsules provide the stability and restraints to this flexible articulated joint. The human finger joint has been frequently imitated and simplified as a hinge joint to develop the implant [9] or robotic/prosthetic hand [10], [11], [12], [13]. However, it is still not clear how the simplified rigid finger joints affect the hand grasping performance and whether the biomimetic flexible joint configuration can improve the robotic hand performance, although it has been found that the flexible bone-on-bone interaction restrained by the soft tissues provides sophisticated passive behavior different from the simplified pin or hinge joint [14], [15]. There is a strong need to understand the biomechanical influences of these rigid joints on hand performance which is critical for the design of the surgical implant and robotic/prosthetic hand.

One of the typical rigid finger joint configurations is the implant introduced by Swanson [16], where the interphalangeal joint is replaced with a silastic hinge during arthroplasty. Metallic hinge-type prosthesis has been developed to replace the metacarpophalangeal or interphalangeal joint affected by the rheumatoid disease. The reliability and biocompatibility of these rigid hinge implants have been well studied [17] while their effects on hand grasping quality and dexterity after surgery have not been quantified and still remain unknown. These physical rigid finger joints have been applied in the prosthetic hand [18] and robotic hands [19], [20] to mimic the kinematics of the human finger. Torsional springs are normally used in the rigid joint to enhance the finger compliance [21], [22] or help to maintain its rest positions [23], [24], [25]. Very few of these physical hand models adopted the flexible joint containing the interphalangeal tissues. Zhe et al. [12] developed a robotic/prosthetic hand with the finger joint containing collateral ligament and volar plate. Hughes et al. [13] constructed a 3D printed soft hand skeleton with a flexible joint consisting of joint capsules and interphalangeal ligaments. However, there are no reports of whether the hand performance is improved after integrating the flexible finger joints and how the joint configurations affect the hand grasping quality. Clearly, these are the crucial pieces of information that need to be explicitly studied for designing better prosthetic robotic hands and surgical implants.

Rigid finger joint configuration has also been widely used in numerical hand models to investigate the biomechanics of

Manuscript received 28 November 2021; revised 14 April 2022, 20 June 2022, and 14 September 2022; accepted 1 November 2022. Date of publication 14 December 2022; date of current version 1 February 2023. *(Corresponding author: Lei Ren.)*

This work involved human subjects or animals in its research. Approval of all ethical and experimental procedures and protocols was granted by the Ethics Committee of the First Hospital of Jilin University.

Yuyang Wei and Zhenmin Zou are with the Department of Mechanical, Aerospace and Civil Engineering, The University of Manchester, M13 9PL Manchester, U.K.

Zhihui Qian is with the Key Laboratory of Bionic Engineering, Ministry of Education, Jilin University, Changchun 130012, China.

Lei Ren is with the Department of Mechanical, Aerospace and Civil Engineering, The University of Manchester, M13 9PL Manchester, U.K., and also with the Key Laboratory of Bionic Engineering, Ministry of Education, Jilin University, Changchun 130012, China (e-mail: lei.ren@manchester.ac.uk).

Guowu Wei is with the School of Science, Engineering and Environment, University of Salford, M5 4WT Salford, U.K. (e-mail: G.Wei@salford.ac.uk).

This article has supplementary downloadable material available at https://doi.org/10.1109/TNSRE.2022.3229165, provided by the authors.

Digital Object Identifier 10.1109/TNSRE.2022.3229165

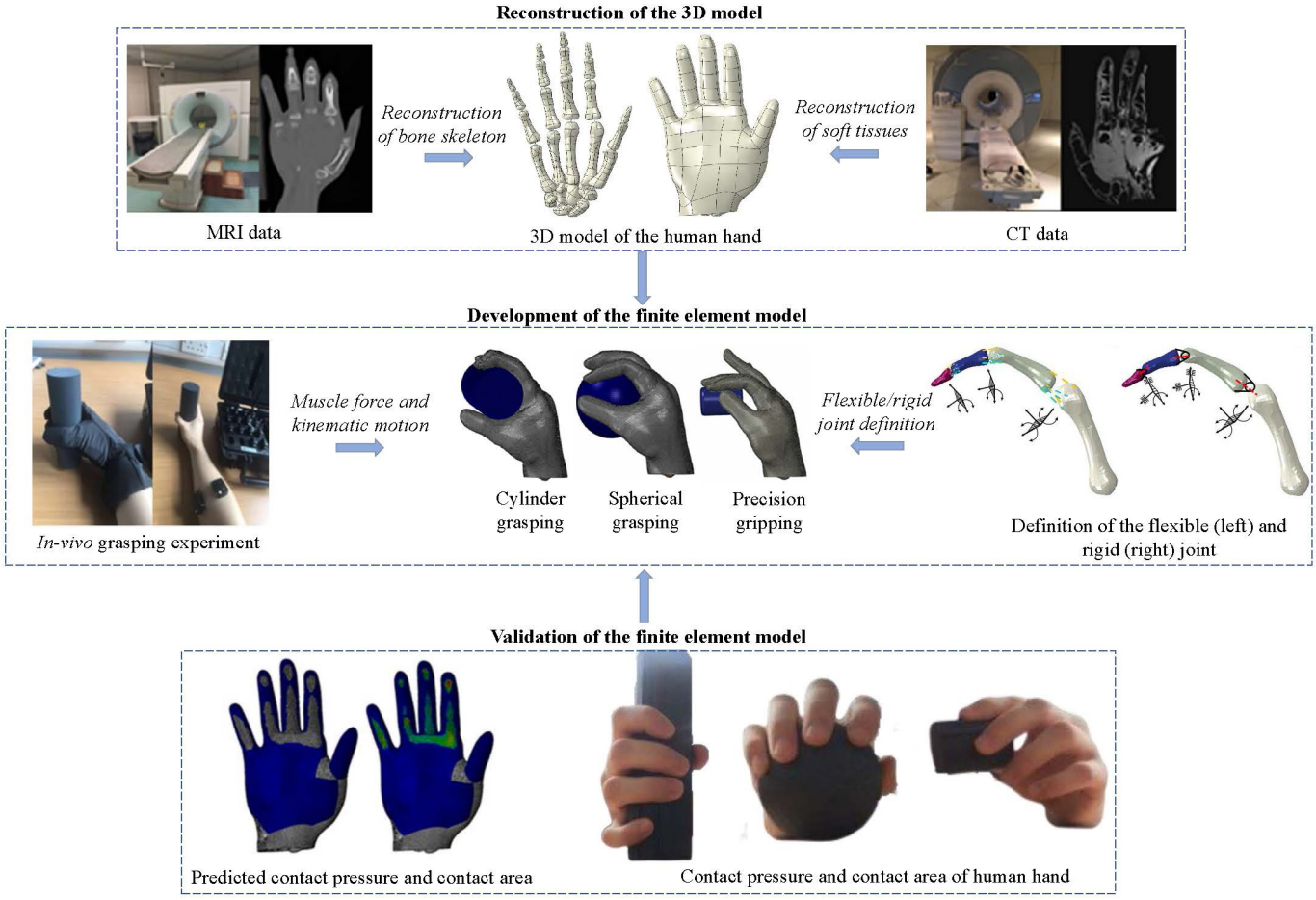

Fig. 1. The main procedure of this study. From CT and MRI data processing to the development of the FE human hand model with flexible or rigid joint configuration. Simulation of three grasping postures to study the biomechanical effects of flexible and rigid finger joint configuration on hand grasping.

finger joint and human hand contact. Very few researchers fully reconstructed the flexible phalangeal joint [26]. Hinge or universal joints are the most frequently used rigid joint to imitate finger joint kinematics. Numerical hand skeleton models with simplified hinge joints were developed to study the biomechanics of the tendon routing [27], musculotendinous force and bone-on-bone load transmission [26], [28], [29]. Anatomically intact numerical hand models were also constructed for understanding the soft contact mechanism and human tactile sensing [30], [31]. However, the effects of these simplified rigid joints on hand performance have not been considered and analyzed in these studies. Undoubtedly, the biomechanics properties of the hand skeleton, the musculotendinous force transmission and the hand contact mechanism will be influenced to some extent due to the adoption of the simplified rigid joint. Accurate representation of the human hand kinematics or biomechanics cannot be achieved by these numerical models with rigid finger joint configuration.

In this study, the superiority of the flexible finger joint over the rigid joint is quantified by using finite element (FE) human hand models with different types of joints. The rigid joint is integrated with the torsional springs to simulate the conventional joint configurations in robotic fingers, and the resulted grasping quality is compared with that of flexible joint configuration. The simulation results show that the grasping quality of robotic/prosthetic hand can be improved significantly by adopting the flexible finger joint configuration rather than the rigid one. The computational hand model with rigid joint configuration underestimates the contact pressure, contact force, contact area and grasping quality of the real human hand.

II. Methods

In our previous study [30], a 23-year-old healthy male was recruited and asked to sit before a table with the wrist being fixed to perform the *in-vivo* grasping experiments including cylindrical, spherical grasping and precision gripping. A cylinder with a diameter of 50 mm and a length of 180 mm was used for cylindrical grasping, a smaller cylinder with a diameter of 35 mm and a length of 50 mm for precision gripping. A sphere with a diameter of 80 mm was employed for spherical grasping. All three objects were 3D printed with Polylactic Acid and are very light. The weight of the heaviest object is less than 15 grams.

The hand kinematics were recorded through the VICON system (Virtual Motion Lab, Dallas, US) and the electromyography (EMG) signals were captured by the Delsys wireless

EMG system (Delsys Inc., Boston, US) during the *in-vivo* grasping test. The captured EMG signal was filtered with a Butterworth filter (20–400 Hz) and rectified. Before the grasping test, maximum voluntary contraction (MVC) tests were carried out for each muscle using the Jamar dynamometer and the muscle forces were then computed based on the MVC forces and the processed EMG signals. A linear relationship between the EMG signal and muscle force for isometric muscle contracting was assumed. A similar method has been used by other researchers to calculate muscle forces under isometric contract [32], [33]. Three main extrinsic muscles associated with hand grasping and the intrinsic thenar muscles were selected for measuring the muscle forces according to hand anatomy and the literature [1], [34]. The subject gave informed consent to participate in the grasping experiments, which were approved by the Ethics Committee of the First Hospital of Jilin University.

The CT/MR images collected from the same subject were used to develop a subject-specific muscle-driven FE human hand model in the commercial FE software ABAQUS(Dassault Systèmes Simulia Corp, Providence, RI). The FE hand model contains the intact hand skeleton, subcutaneous tissue and skin, it can simulate fairly accurate hand biomechanics and contact mechanism. This hand model was validated against experimental data [30].

In the present study (See Fig. 1), this FE hand model is further modified to create FE hand models with flexible and rigid finger joint configurations respectively. Grasping simulations are then conducted to evaluate the grasping qualities under different finger joint configurations.

A. The Flexible and Rigid Finger Joints in the FE Hand Model

The definitions of the flexible and rigid phalangeal joints are shown in Fig. 2. The flexible interphalangeal joint contains the collateral ligaments on the radius/ulna side and the volar plate on the palmar side (see Fig. 2a). Research has shown that joint stability and kinematics are mainly restricted through these two ligaments [26], [35]. The non-linear wire/spring element is applied to model these interphalangeal soft tissues. Such non-linear spring configurations were widely used to represent the soft tissues and good simulation results were achieved [36], [37], [38], [39]. The material properties of the collateral ligament and volar plate are collected from the literature [40] and shown in Table S1 to S3 in the supplementary material. The motion of the flexible joints is assigned by using the angular displacement around the rotation axis while its rotations around the other two axes and the displacements along all directions are unconstrained. Frictionless contact between adjacent phalangeal bones is defined for all finger joints. The rigid hinge and universal joints (see Fig. 2b) are used to simplify the interphalangeal and metacarpophalangeal joints respectively. Similar rigid joint configurations have been adopted in other published computational hand models [29], [31], [41]. The hinge joint strictly fixes the motion of the joint except the flexion/extension while the universal joint only allows the flexion/extension and lateral bending. To simulate the conventional rigid joint configuration adopted in most of the existing robotic/prosthetic hands, one set of torsional springs with the stiffness of 0.027, 0.031 and 0.022 Nm/rad are configured on MCP, PIP and DIP joint respectively. The spring stiffness of 0.049 Nm/rad is used on the CMC joint. These spring stiffnesses are extracted and averaged from the literature [22], [24], [25], [42]. The grasping quality of the FE hand with rigid finger joint is compared with that of flexible joint configuration. The effect of spring stiffness on grasping performance is also investigated.

B. The Grasping Simulation and Model Validation

Cylindrical, spherical grasping and precision gripping are simulated by using the FE hand model with flexible and rigid finger joints respectively. The kinematics and muscle forces applied onto the FE hand models are from the experimental measurements in our previous study on the same human subject [30]. After the FE simulations, the normal contact force, shear contact force, contact pressure and contact area on the hand are extracted and used to assess the hand grasping quality. The typical simulation results of three grasping of the FE hand with flexible and rigid finger joints are shown in Fig. S1 in the supplementary material.

The FE hand model with flexible finger joint configuration is validated against the *in-vivo* grasping experimental results. The contact pressures on fingertips during the grasping experiment were detected by the pressure sensors mounted on the data glove. To measure the contact area of the human hand, red paint was daubed onto the subject's hand and a paper was wrapped onto the surface of the objects to capture the contact area of the hand. The differences between the experimental measured and FE simulated contact pressure, contact area and contact force on each finger of the hand are presented in Table I, II and III. The FE hand model with flexible joint produces slightly lower contact pressures and larger contact areas than the experiment measurements, but with all the relative differences below 10%. However, the predicted contact forces are very accurate, within a 6.2% error range to the experiment forces. The detailed shapes and positions of the contact areas are displayed in Fig. 3, showing that the simulation matches well with the experimental measurement. As expected, the FE hand with rigid finger joints cannot simulate the human hand, producing much smaller contact pressures and contact forces than the experiment results.

The FE hand model with flexible finger joints is further validated against a grasping test of a six-axis force/torque sensor ATI Mini40 (Mini40, ATI Industrial Automation, USA) by the same subject as shown in Fig. S2 in the supplementary material. Due to the size of the six-axis force/torque sensor which is much larger than the thin-film pressure sensors, it is impractical to attach these force sensors onto the fingertip or palm for measurement during grasping. Therefore, the normal and shear contact forces in 3 axial directions on the index fingertip are measured by directly gripping the force sensor. The gripping of the force sensor is then simulated using the FE human hand model with flexible joints. The predicted normal and shear contact forces on the index fingertip are

TABLE I
RELATIVE DIFFERENCE BETWEEN MEASURED AND PREDICTED CONTACT PRESSURE

	Index		Middle		Ring		Little		Thumb	
	Flexible	Rigid	Flexible	Rigid	Flexible	Rigid	Flexible	Rigid	Flexible	Rigid
Cylindrical grasping	-5.25%	-17.25%	-9.07%	-24.29%	-6.90%	-20.86%	-9.07%	-19.76%	-3.82%	-16.15%
Spherical grasping	-5.14%	-21.64%	-7.28%	-25.74%	-3.21%	-20.22%	-5.55%	-21.23%	-5.11%	-17.23%
Precision gripping	-7.47%	-25.09%	-7.25%	-22.86%	N/A	N/A	N/A	N/A	-8.24%	-24.58%

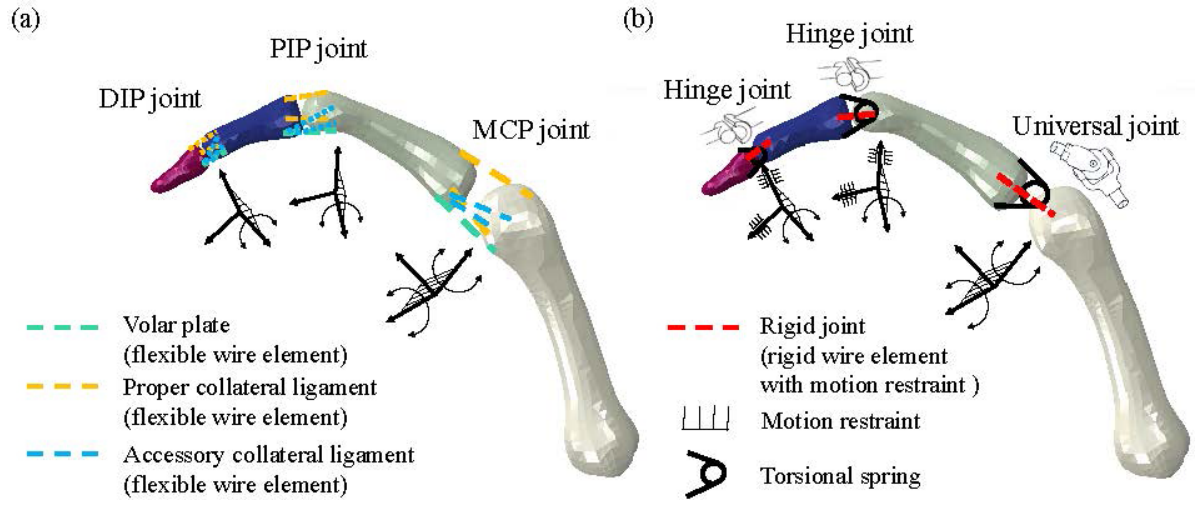

Fig. 2. The flexible and rigid finger joint configurations. (a) The collateral ligament and volar plate are simulated by using the soft wire elements. No rigid constraints are assigned to the flexible finger joints. (b) The hinge and universal joints are assigned to the phalangeal and metacarpal joints respectively. Only the rotation around a specific axis is allowed while the other degree of freedoms of the rigid joints are fixed.

TABLE II
RELATIVE DIFFERENCE BETWEEN MEASURED AND PREDICTED CONTACT AREA

	Index		Middle		Ring		Little		Thumb	
	Flexible	Rigid	Flexible	Rigid	Flexible	Rigid	Flexible	Rigid	Flexible	Rigid
Cylindrical grasping	4.46%	-4.61%	4.50%	-5.44%	4.28%	-5.43%	3.49%	-3.54%	4.04%	-4.19%
Spherical grasping	5.47%	-5.85%	3.71%	-4.21%	4.62%	-4.77%	3.61%	-3.72%	3.89%	-4.23%
Precision gripping	4.86%	-5.02%	4.62%	-5.53%	N/A	N/A	N/A	N/A	4.17%	-4.42%

TABLE III
RELATIVE DIFFERENCE BETWEEN MEASURED AND PREDICTED CONTACT FORCE

	Index		Middle		Ring		Little		Thumb	
	Flexible	Rigid	Flexible	Rigid	Flexible	Rigid	Flexible	Rigid	Flexible	Rigid
Cylindrical grasping	-1.02%	-21.06%	-4.98%	-28.41%	-2.92%	-25.16%	-5.90%	-22.60%	0.07%	-19.66%
Spherical grasping	0.05%	-26.22%	-3.84%	-28.87%	1.26%	-24.03%	-2.14%	-24.16%	-1.42%	-20.73%
Precision gripping	-2.97%	-28.85%	-2.96%	-27.13%	N/A	N/A	N/A	N/A	-4.41%	-27.91%

Note: The relative differences of the magnitudes for the contact parameters between the FE hand with flexible/rigid joint and human hand are listed. The contact pressure and contact area are compared in terms of the five fingers separately, the left column stands for the differences between the FE hand with flexible finger joint and experiment measurement, while the right column represents those under rigid joint and torsional springs with the similar stiffness to those adopted in robotic hands.

in good agreement with the measured forces, with the relative differences being below 8% (See Table S4).

C. The Evaluation of the Grasping Quality

Three types of grasping quality measures are used in this study: (1) The limits of the finger forces which is related to contact forces; (2) The geometric relations of the grasp which relate directly to the contact area (size and shape); (3) The algebraic properties of grasping matrix **G** which depends upon contact forces and moments. The contact moments are related to both contact forces and areas. Therefore, it represents the combined effect of contact areas and forces. These three

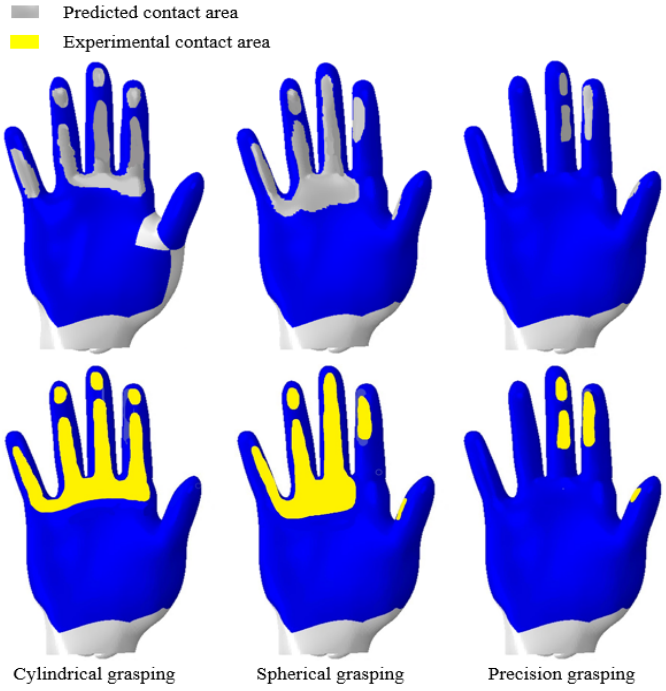

Fig. 3. Comparison of contact area between experimental measurement and FE prediction. The grey zone represents the predicted hand contact area (first row) while the yellow zone represents the measured hand contact area (second row).

types of grasping quality measures show a comprehensive assessment of the hand grasping quality which have been used by researchers [43], [44], [45].

From the finite element simulations of the cylinder, spherical grasping and precision gripping, the following results can be extracted as the database for the derivation of the grasping quality: (a) The contact areas on each finger. (b) The three components of the contact force, F_x, F_y and F_z, on the contact surface of the grasped object. (c) The three components of the contact moment, M_x, M_y and M_z, about the three coordinate axes on the surface of the grasped object. (d) The three contact force components, f_{xi}, f_{yi} and f_{zi}, on the surface of the i-th finger, the moment m_{zi} around axis z.

The external wrench $\boldsymbol{w}$ on the grasped object is then obtained as $\boldsymbol{w} = [F_x\ F_y\ F_z\ M_x\ M_y\ M_z]^T$. The internal wrench $\mathbf{f_c}$ is defined as $\boldsymbol{f_c} = [f_{x1}\ f_{y1}\ f_{z1}\ m_{z1}\ \ldots\ldots f_{xn}\ f_{yn}\ f_{zn}\ m_{zn}]^T$. Finally, the internal wrench $\mathbf{f_c}$ is related to the external wrench $\boldsymbol{w}$ by the grasping matrix $\boldsymbol{G}$ as follows [43]:

$$-\mathbf{w} = \boldsymbol{G} * \boldsymbol{fc} \tag{1}$$

Since $\boldsymbol{w}$ and $\boldsymbol{f_c}$ are already obtained from FE simulation, $\boldsymbol{G}$ is determined from the above equation.

Based on the grasping matrix $\boldsymbol{G}$ and the contact areas and forces, the following indices are employed in this study to evaluate the grasping quality.

1) Minimum Singular Value of **G***:*

$$Q_{MSV} = \sigma_{min}(\boldsymbol{G}) \tag{2}$$

The grasp becomes unstable when one of the singular values turns to zero and the hand will lose the capability for balancing the wrench at least in one direction. $\sigma_{min}(G)$ indicates how far the grasp configurations is from the singular configuration [43].

2) Volume of the Ellipsoid in the Wrench Space:

$$Q_{VEW} = \sqrt{det(\boldsymbol{G}\boldsymbol{G}^{\mathbf{T}})} \tag{3}$$

The grasp matrix $\boldsymbol{G}$ maps a sphere of unitary radius in the force domain of the contact points into an ellipsoid of the wrench space. Q_{VEW} should be maximized to obtain the optimum grasp [43].

3) Grasp Isotropy Index: The grasp isotropy index is defined as:

$$Q_{GH} = \frac{\sigma_{min}(\boldsymbol{G})}{\sigma_{max}(\boldsymbol{G})} \tag{4}$$

$\sigma_{min}(\boldsymbol{G})$ and $\sigma_{max}(\boldsymbol{G})$ are the minimum and maximum singular values of $\boldsymbol{G}$. A more uniform contribution of the contact forces to the total wrench applied on the object and a more stable grasp can be achieved when the value of Q_{GH} is close to 1 [43].

4) Area of the Grasp Polygon Q_{AGP}: A larger contact area on the object produces a more robust grasp since the grasp can resist a larger external wrench with a bigger contact area under the same contact forces [43].

5) Distance Between the Centroid of the Contact Polygon and the Object's Center of Mass Q_{DCC}: A shorter distance contributes to a better grasping quality [43].

6) Largest-Minimum Resisted Wrench:

$$Q_{LRW} = \|\boldsymbol{w}\| \tag{5}$$

The magnitude of the perturbation wrench that the grasp reaches under the maximum voluntary contraction forces (MVC) is defined as Q_{LRW} in this study. A larger value of Q_{LRW} means a more stable grasping [43].

7) Normal Components of the Forces:

$$Q_{MNF} = \min \frac{1}{\sum_{i=1}^{n} \boldsymbol{f_i^n}} \tag{6}$$

Q_{MNF} should be minimized to optimize the grasp [43], as larger normal components of these forces represent more efficient grasp.

Among the above grasping quality indices, indices Q_{MSV}, Q_{VEW} and Q_{GH} are related to the measure of the algebraic properties of grasping matrix $\boldsymbol{G}$. Indices Q_{AGP} and Q_{DCC} are based on the geometric relations of the grasp. Indices Q_{LRW} and Q_{MNF} consider the limits of the finger forces. These grasping quality quantifying standards follow the grasp quality measures in the review paper by Roa et al. [43] and are explained in more details in [46].

D. The Contact Feasible Force Set and Finger Stiffness

The feasible force sets (FFS) of the fingertip contact forces are computed based on the same grasping simulation but under different input of muscle forces according to Minkowski sum algorithm [47]. There are up to five muscle forces that can be applied to the fingers in the hand model, resulting in 31 combinations of these muscle forces to compute the FFS

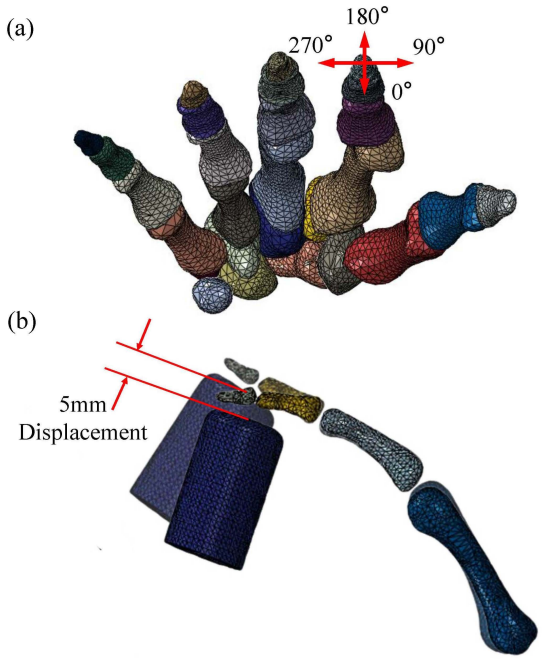

Fig. 4. The simulation for calculating finger stiffness. (a) The coordinate for defining the direction of the stiffness together with the hand skeleton. (b) The simulation procedure for measuring the index finger stiffness from the direction of the angle 0°. The MCP joint is fixed while the cylinder is used to push the index finger to a displacement of 5mm.

(5 individual forces, 10 different combinations of any two muscle forces, 10 different combinations of any three muscle forces, 5 different combinations of any four muscle forces and 1 for all five muscle forces). The hand contact outputs (contact forces along the three axis of the local coordinate) are computed under each of these different muscle force inputs and the convex hull of the FFS is then drawn using Minkowski sum algorithm.

The stiffness of the index finger and the thumb with the flexible and rigid finger joints are also determined to study the effects of the two different joint configurations. Fig. 4 illustrates how the stiffness of the index finger is computed. The MCP joint is fixed, and a cylinder is used to push the finger in a specified direction to a distance of 5mm. The simulated relationship between the contact force on the fingertip and displacement of the cylinder is plotted. A line is then fitted to these data points and the slop of this line is regarded as the finger stiffness. Similar method was used by other researchers for determining the stiffness and impedance of the joint and finger [13], [48], [49], [50]. More simulation scenarios are illustrated in Fig. S3 in the supplementary material. The stiffness in different directions with and without actuating muscle forces is calculated.

III. Results

The contact pressure, contact area, normal and shear contact forces are extracted from the simulation results. The FE hand with a flexible finger joint is regarded as the baseline model. Fig. 5 presents the changes to the contact parameters and grasping qualities of the FE hand caused by the rigid joint with torsional springs similar to most of the published robotic hands with respect to the baseline model under cylindrical, spherical grasping and precision gripping. Reductions are found in contact pressure, contact area, contact force and grasping quality compared with the baseline model under all three grasping postures, resulting in the distorted convex hull of FFS and anisotropic joint stiffness as shown in Fig. 6 and Fig. 7 respectively under rigid finger joint configuration.

The use of rigid joint reduces the grasping quality by more than 36% in terms of algebraic properties of grasping matrix (see Fig. 5a). The geometry relation based grasping quality is least affected, only less than 12% of reduction. Among the three grasping postures, the precision gripping is the one most sensitive to the adoption of rigid finger joint, evidenced by the observation that the grasping quality indices are decreased more during precision gripping than the power grasping. The detailed variations of the grasping quality evaluation indexes are presented in Tables S5-S7 in the supplementary material. The variations of contact pressure, contact area and contact force on the whole hand and each individual finger are shown in Fig. 5b and Fig. 5c respectively. Normal contact forces are decreased by 19% under cylindrical grasping, over 20% reductions are observed during spherical grasping and precision gripping. Significant reductions in the contact forces, pressure and area occur on the thumb, index and middle fingers during power grasping. Reductions less than 20% in the four contact parameters are found on the little and ring fingers. The fingertip contact pressure and force are affected more in precision gripping than in the power grasping, resulting in the more severe shrinking of the convex hull of FFS and then the reduction of grasping quality. The FFS for each grasping with two different joints configurations is presented in Fig. 6. Larger and more even convex hulls of the FFS are achieved by the FE hand with flexible joint than that of the rigid one. The reduced fingertip contact forces are responsible for the shrinking of the convex hull for the FFS of the hand with a rigid joint.

Fig. 7 presents the finger stiffness of the flexible joint in different directions. The stiffness distribution of the finger with rigid joint configuration and torsional springs with the stiffness of 0.027, 0.031, 0.022, 0.049 Nm/rad on MCP, PIP, DIP and CMC joint (similar spring stiffness to those adopted in robotic hand) are also presented. It can be seen that the finger with a rigid joint is much stiffer than that with flexible joint, but not in the rotation direction of the hinge and universal joints. The rigid joint increases the finger stiffness up to approximately four times larger than those of the flexible one. Similar finger stiffness variation is observed when the fingers are under the actuation of the muscles. As expected, the index finger is stiffer in radius and ulna side, while the thumb is stiffer in the ulna and palmar direction than in the other directions. The index finger and the thumb under two different finger joint configurations display anisotropic stiffness behavior. It is critical to notice that the finger with a flexible joint is much stiffer than that with the rigid joint in the motion of flexion/extension or lateral bending.

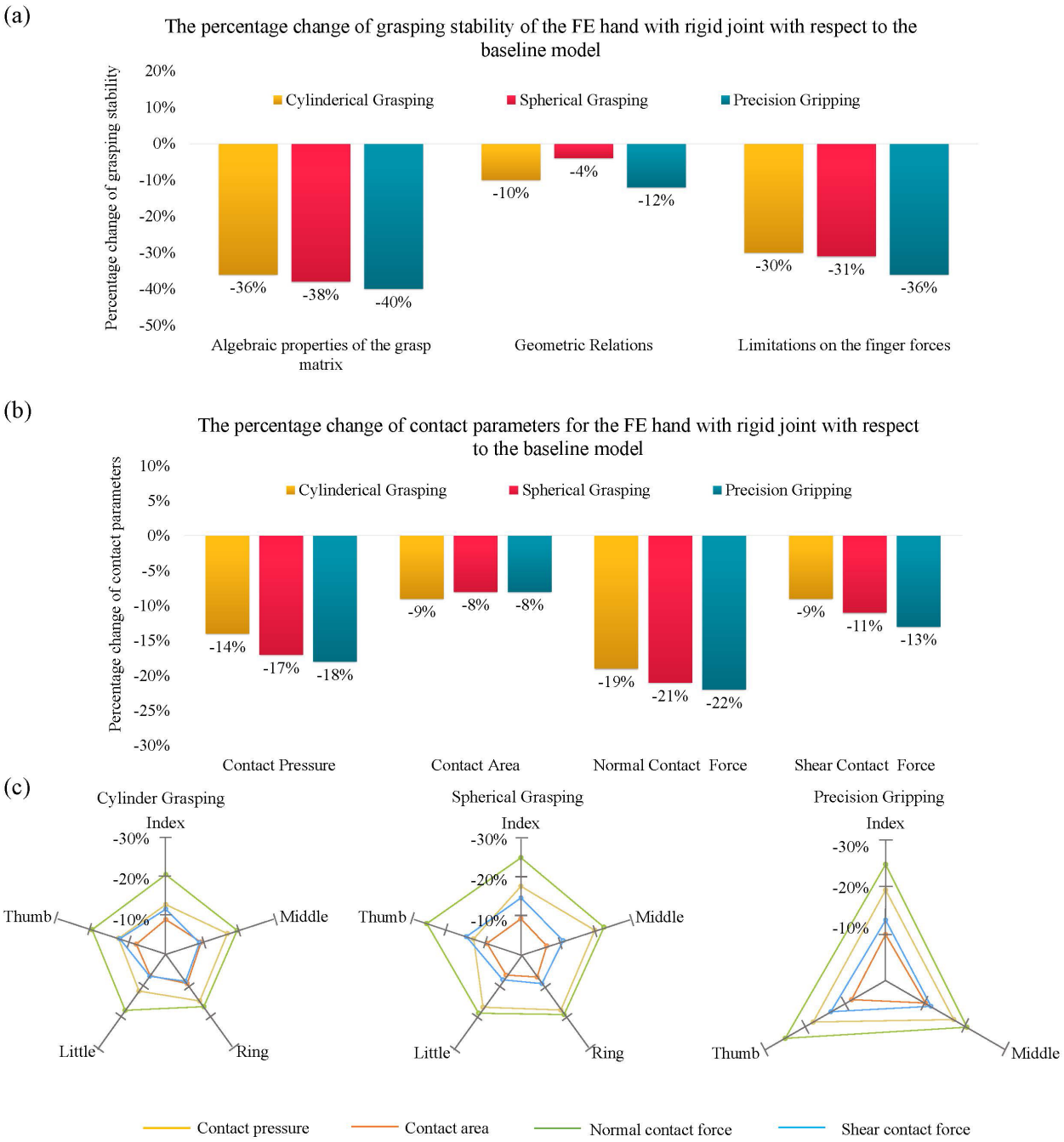

Fig. 5. The percentage changes of grasping qualities and contact parameters of the FE hand with rigid joint with torsional springs similar to most of the published robotic hands with respect to the baseline model with flexible joint. (a) The changes of grasping qualities. (b) The changes of contact pressure, area and force on the hand. (c) The variations of the contact pressure, area and force on the fingertips. The grey regular pentagons and triangles are the scales of the differences.

It is obvious that the finger stiffness under the rigid joint configurations is affected by the torsional springs. The very low stiffness of the torsional springs used in the aforementioned simulations may be the reason for the much lower finger stiffness than the human finger and contributes to the undesirable hand performance of the FE hand with the rigid joint. Therefore, it is necessary to further assess the grasping quality of the rigid joint hand when the finger stiffness is comparable with the human subject. Efforts are then made to modulate the stiffness of the torsional springs in the rigid joint so that the stiffness of each finger is increased and made very close to the human finger in the direction resisting the motion of flexion. To simplify the stiffness modulation, the same spring stiffness is used on the individual rigid finger, but different spring stiffness among the different fingers. The modulated spring stiffnesses thus obtained are 0.316, 0.293, 0.237, 0.158 and 0.326 Nm/rad on the joints of index, middle, ring, little and thumb respectively. These stiffnesses are at a similar level as those used/reported in the literature [51], [52], [53]. Fig.8 shows the grasping quality of the hand with the

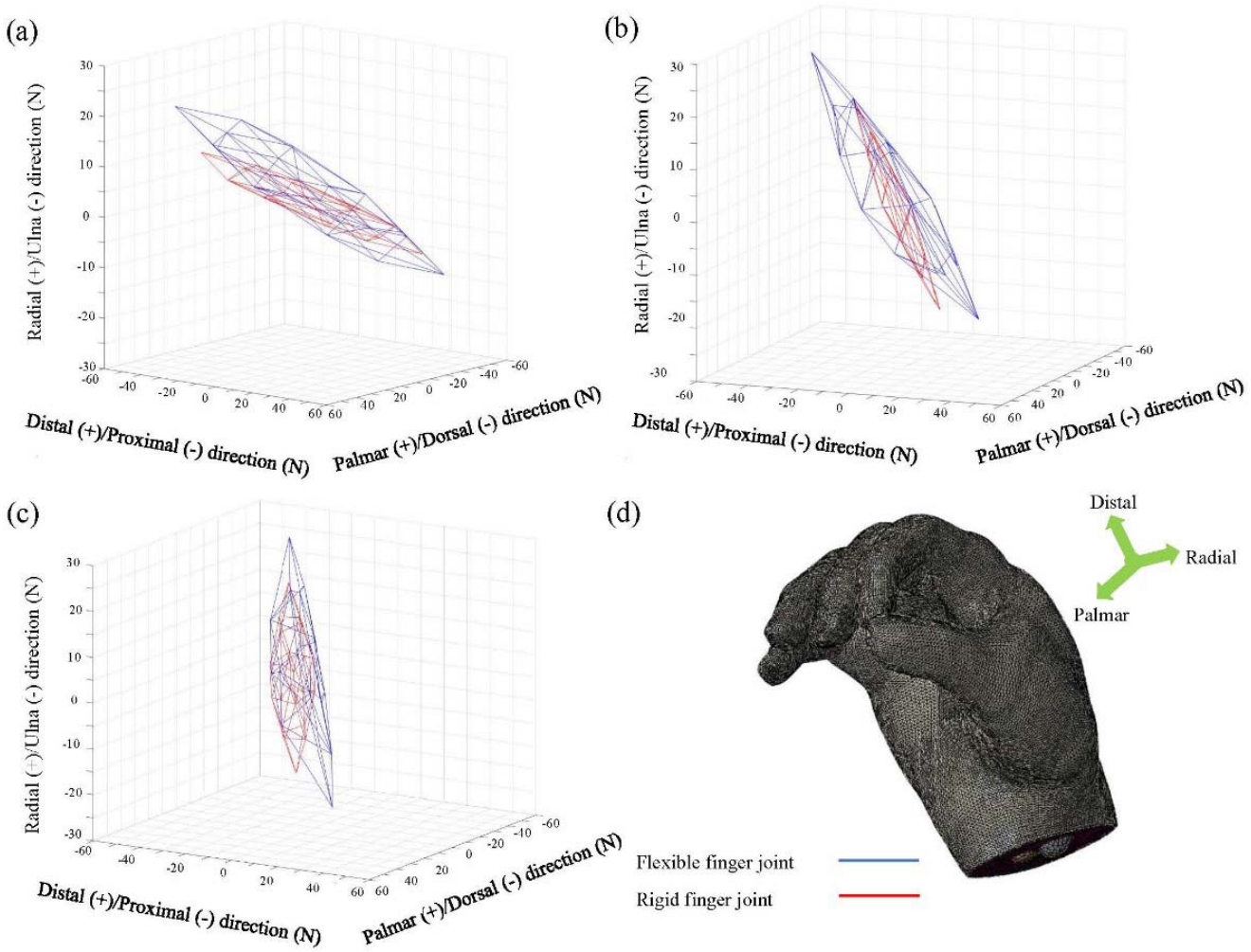

Fig. 6. Fingertip contact feasible force sets for the FE hand with rigid and flexible joints. (a) FFS for cylinder grasping. (b) FFS for spherical grasping (c) FFS for precision gripping. (d) The anatomical position defined for the FFS diagram. The volume of FFS under flexible finger joint is larger than that under rigid joint in terms of all grasping postures, indicating that a firmer grasping is achieved under flexible finger joint configuration.

rigid joint adopting these torsional springs. It can be seen that the grasping quality is improved, but this hand is still inferior to the hand adopting flexible finger joints. There are still more than 15% reduction in the algebraic properties of grasp matrix, up to 23% shrinking with respect to the limitations on finger forces and less than 8% reduction in the geometric relation. This is because the stiffness increase of the torsional springs decreases the reductions in the contact parameters, e.g., the reduction of the contact pressure is reduced to 9%, 10% and 11% in cylindrical, spherical and precision grasping respectively, in comparison to the 14%, 17% and 18% reductions caused by the springs of lower stiffness shown in Fig. 5(b). The detailed variations of the grasping quality evaluation indexes and the stiffness distribution of the rigid finger are presented in Tables S8-S10 and in Fig. S4 in the supplementary material.

In summary, the numerical simulations show that the human flexible finger joint is superior to the rigid one used in robotic/prosthetic hands in all aspects, even when the stiffness of the rigid joints is increased to the similar level to the human subject.

IV. Discussions

The rigid hinge and universal joints have been widely applied in robotic, biomimetic and even computational hands to represent the flexible phalangeal joint [10], [11], [12], [27], [30], [49]. Some of the physical rigid joints were integrated with the torsional springs to enhance the compliance [21], [22] or help to maintain its rest position [23], [24], [25]. Whether the kinematics and biomechanical properties of the human hand can be restored through this simplified joint is still not clear. The effects of this rigid joint configuration on hand dexterity and grasping quality haven't been quantified, although these are critical information for developing finger implant, robotic/prosthetic hand and computational hand model. In this study, the superiority of the flexible finger joint over the rigid one is quantified through a FE human hand model. It is observed that flexible finger joint configuration enables larger contact parameters than the rigid joint with a lower or even similar joint stiffness, leading to a larger and even convex hull of the FFS and moderate isotropic finger stiffness. All these better parameters finally contribute to a higher grasping quality.

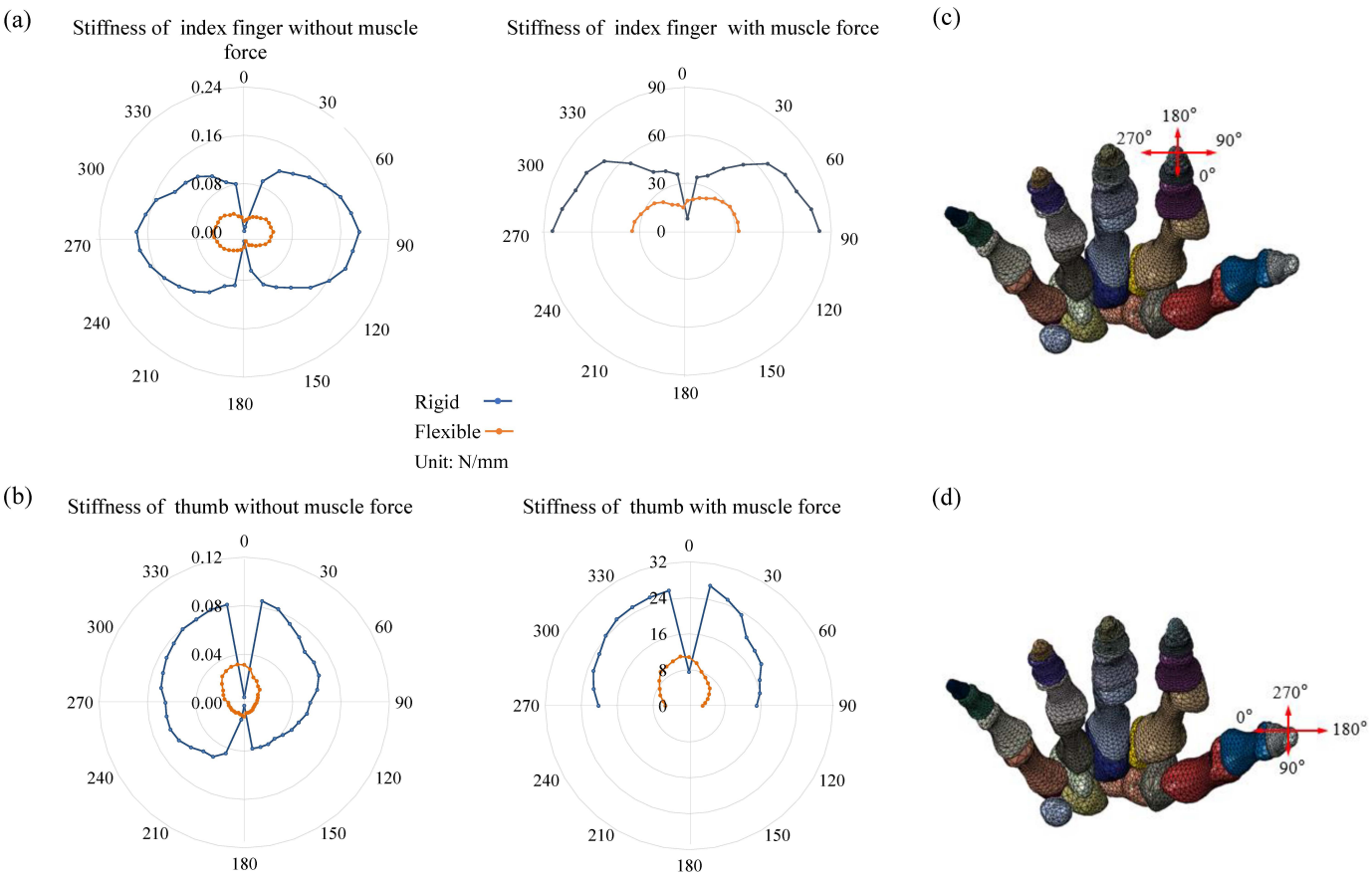

Fig. 7. The simulated stiffness (unit N/mm) of different fingers. (a). The simulated stiffness of the index finger integrating the torsional springs with similar stiffness adopted in robotic hand. The stiffness in different directions with and without actuating muscle forces are all calculated and shown in the radar plots. The finger stiffness under muscle forces is only measured from directions of palmar side or against the flexor muscle forces (0-90°, 270-360°◁, the stiffness toward the direction of flexor muscle forces (90-270°◁ are not considered in this study. The rotational direction of the torsional spring is toward to the direction of 180°. (b). The simulated stiffness of the index finger. (c). The directions for calculating the stiffness of the index finger. (d). The directions for calculating the stiffness of the thumb.

The use of conventional rigid hinge/universal joint with torsional springs adopted in robotic hands reduces the hand grasping quality significantly due to its adverse effect on the contact parameters. The numerical results show that the normal contact forces are reduced by more than 19% and shear force by more than 9% after adopting the rigid finger joint with torsional springs similar to those in robotic hands. The contact pressure and contact area are decreased as well. Lower contact pressure and smaller contact area achieved by the rigid hinge finger joint configuration lead to loose and less stable contact between the hand and the object. Fig. 5c presents the variation of contact force on each fingertip. Large reductions in the normal and shear contact forces are observed on index, middle and thumb fingers. The use of torsional springs in the rigid joint hand whose finger stiffness is comparable with the human subject improves the magnitudes of the contact parameters. However, the contact pressure and contact force are still more than 9% smaller than those under flexible joint configuration and the contact areas are about 5% less as shown in Fig. 8b.

The algebraic properties of grasping matrix and finger force limits are directly related to the contact force and contact area. Reduced contact pressure, contact area and contact force by the use of rigid joint (See Fig. 5b) lead to the distorted wrench space and then contribute to the reduced algebraic properties of grasp matrix and finger force limitations. This explains why the grasping quality associated with the algebraic properties of the grasping matrix may lose up to 40% and the finger force limits based grasping quality lose more than 30% due to the use of rigid finger joints. Fig. 5a also shows that the least affected grasping quality index is the geometry relation. This is due to the fact that geometry relation is directly associated with the contact area which is the least affected among all the contact parameters as shown in Fig. 5b. In particular, the grasping quality associated with the geometry relation is reduced by only 4% during spherical grasping. This is due to the fact that the distance between the centroid of the contact polygon and the sphere's center of mass is not affected by the different joint configurations. The percentage change of Q_{DCC} (one of the sub-indices of geometric relations) is zero. On the contrary, precision gripping is very sensitive to the use of the rigid joint configuration, losing more grasping quality than the other grasping postures. This echoes the finding that significant reductions occur in contact pressure, contact area and contact forces on the three radial fingers that are involved in precision gripping as shown in Fig. 5c. This leads to a larger shrinking of the convex hull of FFS and reduction in grasping

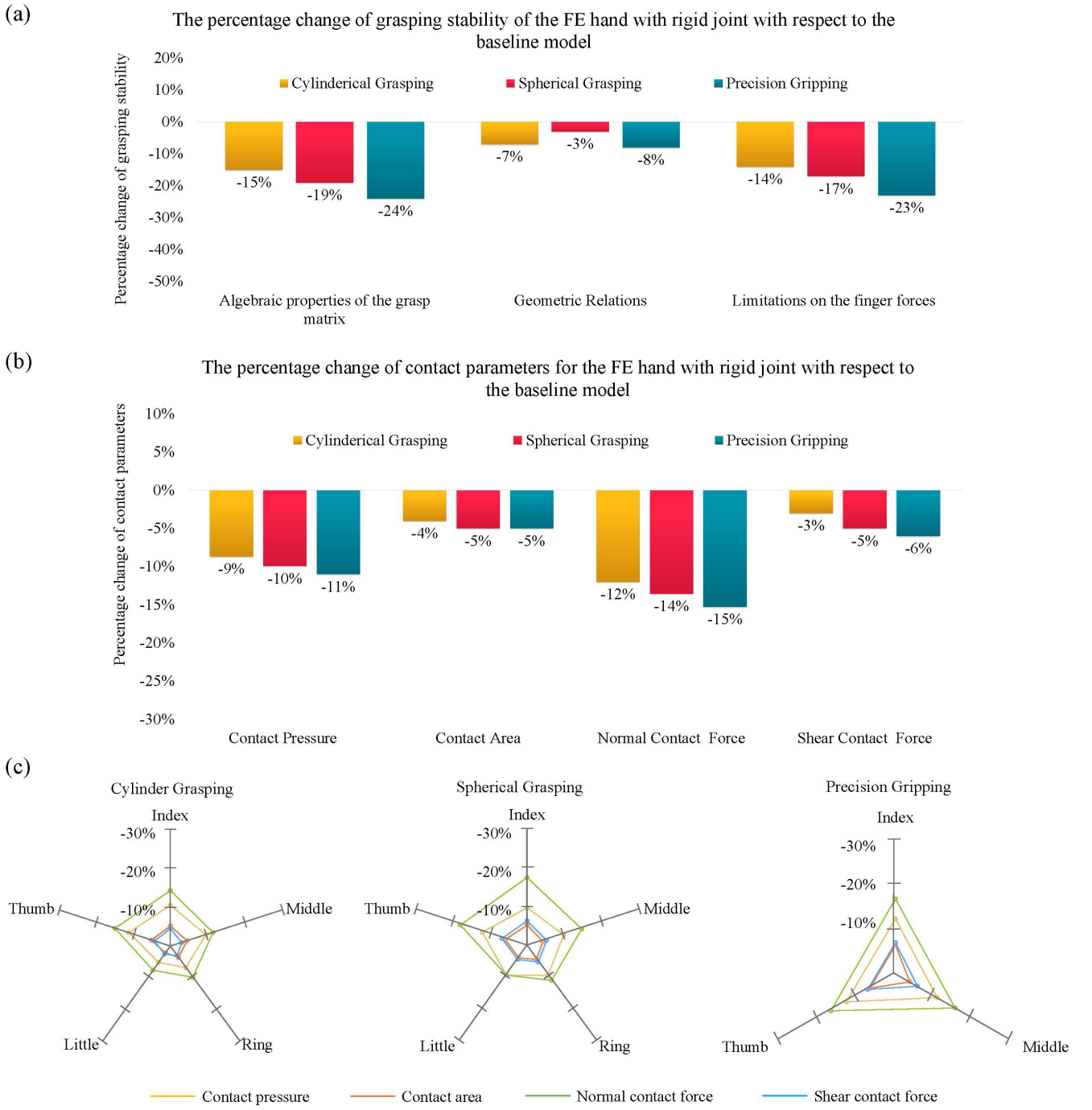

Fig. 8. The percentage changes of grasping qualities and contact parameters of the FE hand with torsional springs possessing the stiffness equivalent to human finger compared with the baseline model with flexible joint. (a) The changes of grasping qualities. (b) The changes of contact pressure, area and force on the hand. (c) The variations of the contact pressure, area and force on the fingertips. The grey regular pentagons and triangles are the scales of the differences.

quality than power grasping where all five fingers and the palm are involved.

The contact force between the hand and the object is the gripping force applied by the hand to the object and the reaction force from the object to the hand. During the gripping, the ability of the finger to resist the reaction force from the grasped object is the key to the grasping quality. If the finger is too flexible, then it is hard to produce a large gripping force and high grasping quality. When grasping an object, the rotation of the fingers around their joints is the main movement of the hand so that a large contact area and grasp polygon can be produced. To achieve a large grasping force, the finger should be able to resist the rotation movement caused by the contact force on it.

The effect of finger stiffness on grasping performance is further investigated by varying the stiffness of the torsional springs in the rigid joint based on those configured in Fig. 8. The original stiffnesses (0.316, 0.293, 0.237, 0.158 and

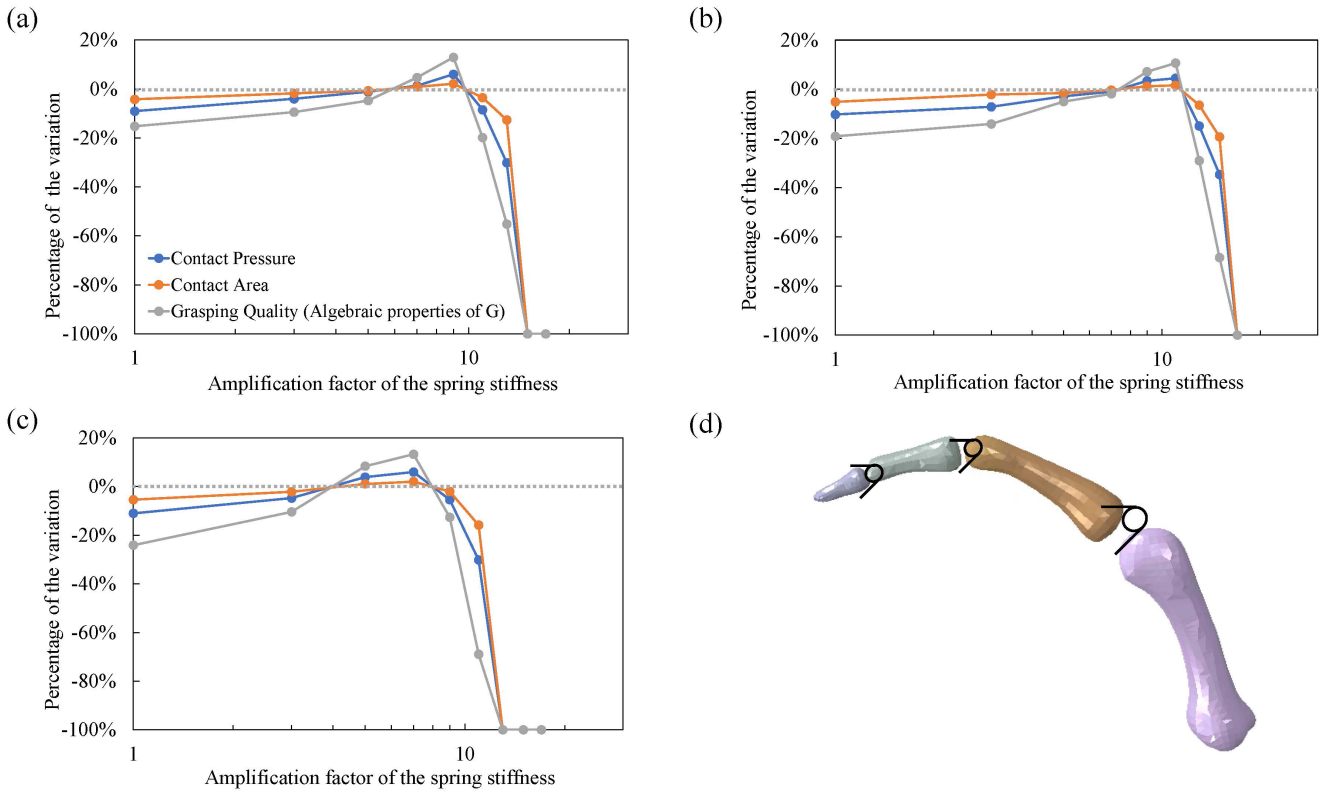

Fig. 9. The percentage changes of the contact parameters and grasping qualities of the FE hand under rigid joint configuration with torsional springs compared to that under flexible joint configuration. The torsional springs are configurated at the DIP, PIP and MCP joint to enhance the stiffness of the finger and to see whether the contact pressure, contact area and grasping quality could be improved by increasing finger stiffness. The stiffnesses of the springs were multiplied from 1 to 17 (logarithmic in the diagram) based on those configured in Fig. 8 (0.316, 0.293, 0.237, 0.158 and 0.326 Nm/rad on the joints of the index, middle, ring, little and thumb). (a) Cylindrical grasping. (b) Spherical grasping. (c) Precision gripping. (d) The configuration of the torsional springs.

0.326 Nm/rad on the joints of the index, middle, ring, little and thumb) were multiplied by an amplification factor ranging from 1 to 17. The obtained variations of contact pressure, contact area and grasping quality are shown in Fig. 9. As expected, increasing the stiffness of the torsional springs in the rigid joint enhances hand performance. However, to achieve a grasping quality similar to the flexible joint, a very high spring stiffness around 7 times of their original stiffness is required, much stiffer than those adopted in most of the published robotic hands [21], [22], [23], [24], [25]. Over-stiffened torsional spring reduces the contact pressure, contact area, and subsequently the grasping quality, echoing the finding in the literature that the robotic finger with a too large stiffness is not ideal for controlling and maintaining high dexterity on robotic or prosthetic hands [23]. A large amount of the muscles will be needed to overcome the rotation resistance of the very stiff fingers, rather than to grasp the object. When the spring stiffness approaches 17 times their initial values, the muscle force cannot actuate those stiff fingers to perform the grasping at all, and the contact parameters and grasping quality are dropped to zero, resulting in a '−100% decrement' of the contact parameters as shown in Fig. 9. Therefore, optimization is needed to achieve a trade-off between the gasping quality and control difficulty when adopting torsional springs in robotic hands.

The rigid joint configuration with similar finger stiffness to the flexible finger joint still present grasping quality inferior to that of the flexible joint configuration. This could be explained by the fact that fingers with flexible joints possessing similar stiffness in all directions due to the combined constraints from the collateral ligaments on the radius/ulna side and the volar plate on the palmar side. On the other hand, the finger with rigid hinge and universal joints is very stiff in other directions, because these mechanical joints strictly constrain the motions of the finger except the flexion/extension and adduction/abduction. Therefore, the pronation and supination of the finger during hand grasping can hardly be performed under the rigid joint configuration while this motion is critical for maintaining precision control and hand dexterity [54], [55]. In contrast, the finger with a flexible joint has moderate and approximately isotropic stiffness. Hence, this finger with a flexible joint can move in all directions without much difficulty, enabling the hand with a higher dexterity compared with the rigid configuration with similar joint stiffness. Similar isotropic finger stiffness was reported in [13].

Finally, the effect of the ligament stiffness of the flexible finger joint configuration on grasping quality was also studied. The forces in the force-displacement data of the interphalangeal ligaments were multiplied by a factor ranging

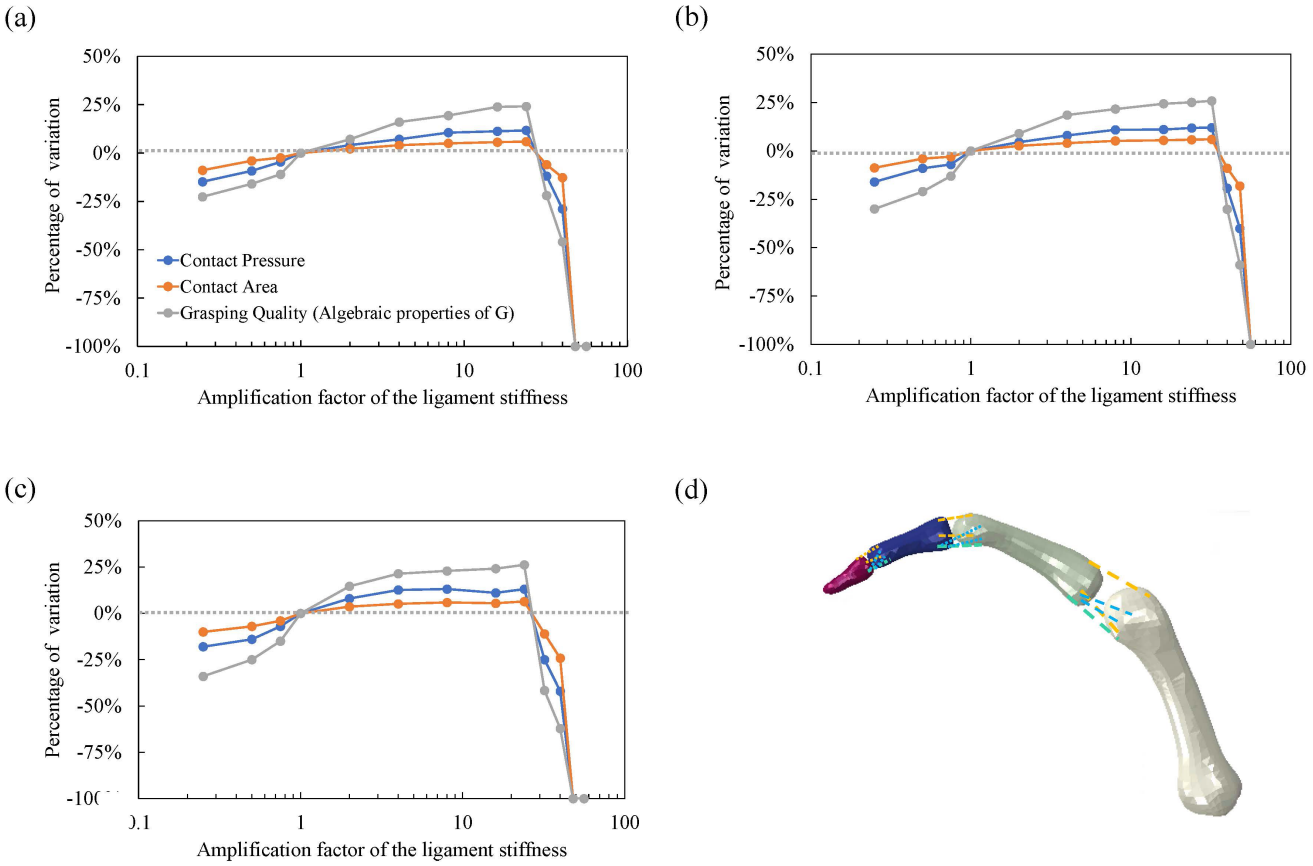

Fig. 10. The percentage changes of the contact parameters and grasping qualities of the FE hand under flexible joint configuration with modified stiffness of the ligaments. The force of the force-displacement data defining the interphalangeal ligaments was amplified by the factors ranging from 0 to 56 (logarithmic axis). (a) Cylindrical grasping. (b) Spherical grasping. (c) Precision gripping. (d) The configuration of the springs for simulating the ligaments.

from 0.25 to 56. The resulting contact pressure, contact area and grasping quality were computed and compared with the baseline model as shown in Fig. 10. The hand performance became worse than the FE hand adopting rigid finger joint when the stiffnesses of the ligaments were reduced to 25% of their original magnitudes. The contact pressure, contact area and grasping quality increased with the hardening of ligaments, but the improving rate slowed dramatically after the amplification factor was larger than 6. The grasping quality became insensitive to the ligament stiffness in a wide range between 6 times and 24 times its original magnitudes. This enables an easy stiffness modulation for the robotic finger if adopting the flexible joint configuration. When the ligament becomes very stiff (48 times their initial values), the muscle force cannot actuate those stiff finger joints, leading to a '−100% decrement' of the contact parameters and grasping quality as shown in Fig. 10.

All the results and above demonstrate that the flexible finger joint is superior to the rigid one when used in the hand. The flexible joint provides the fingers with a high grasping quality but with a reasonable stiffness to resist the finger rotation. It may be crucial to have the flexible joint design in robotic/prosthetic hands by integrating flexible constraint such as artificial ligaments or capsules, so that they can restore human-like hand performance. It is believed that the use of rigid joints in the computational hand models in the literature would have underestimated the performance of the real human hand.

The grasping performance of the FE hand with rigid finger joints are assessed against the data from the flexible joint configuration. It would be ideal to use experimental data as the benchmark for comparison if they could all be measured during the gasping tests. Unfortunately, only the contact areas and normal contact pressures can be measured by using the current technology. It is difficult to attach the force sensors onto the fingertips or palm during grasping to measure other parameters due to their large size. Therefore, it is unrealistic to obtain all the grasping quality indices through experimental measurements and use them as the benchmark for comparison. This is the reason why the finite element hand model with flexible joint is used as the benchmark model. The validation shows that the predicted contact areas and contact forces by this FE hand model both have an error of less than 6% compared to the experimental measurements. The grasping quality indices obtained from this FE hand model can represent the human hand performance with a good accuracy. Future work can focus on simulating more grasping scenarios and gain a deeper and more comprehensive understanding of the effects of finger joint configurations on hand grasping quality.

V. Conclusion

A subject-specific FE human hand model was employed to quantify the biomechanical effects of the rigid finger joint configuration on hand performance. The grasping quality, finger stiffness and the contact parameters including contact pressure, contact area and contact force were evaluated based on the FE hand with flexible and rigid joint configurations. It was found that the adoption of the rigid joint design with torsional springs in most of existing robotic hands reduced the contact parameters and subsequently the grasping quality significantly compared to the hand with flexible joint. It would be better to use flexible finger joint configuration in robotic/prosthetic hands to enable good grasping quality and dexterity. The results indicated that more accurate contact mechanisms in the human hands can only be achieved by using the flexible joint rather than the rigid one based on the proposed computational hand model.

Acknowledgment

The authors acknowledge The University of Manchester for providing the computing resources. They also want to thank Dr. Zhuo Wang from The First Bethune Hospital of Jilin University for offering MRI and CT scanners.

Conflict of Interest

The authors declare that they have no conflicts of interest.

References

[1] C. L. Taylor and R. J. Schwarz, "The anatomy and mechanics of the human hand," *Artif. limbs*, vol. 2, no. 2, pp. 22–35, May 1955.

[2] W. W. Dzwierzynski, H. S. Matloub, J.-G. Yan, S. Deng, J. R. Sanger, and N. J. Yousif, "Anatomy of the intermetacarpal ligaments of the carpometacarpal joints of the fingers," *J. Hand Surgery*, vol. 22, no. 5, pp. 931–934, Sep. 1997.

[3] N. Berme, J. P. Paul, and W. K. Purves, "A biomechanical analysis of the metacarpo-phalangeal joint," *J. Biomech.*, vol. 10, no. 7, pp. 409–412, Jan. 1977.

[4] E. Chao, J. Opgrande, and F. Axmear, "Three-dimensional force analysis of finger joints in selected isometric hand functions," *J. Biomech.*, vol. 9, no. 6, p. 387, 1976.

[5] N. Brook, J. Mizrahi, M. Shoham, and J. Dayan, "A biomechanical model of index finger dynamics," *Med. Eng. Phys.*, vol. 17, no. 1, pp. 54–63, Jan. 1995.

[6] M. Tomaino, G. Mitsionis, J. Basitidas, R. Grewal, and J. Pfaeffle, "The effect of partial excision of the A2 and A4 pulleys on the biomechanics of finger flexion," *J. Hand Surgery*, vol. 23, no. 1, pp. 50–52, Feb. 1998.

[7] K. D. Butz, G. Merrell, and E. A. Nauman, "A biomechanical analysis of finger joint forces and stresses developed during common daily activities," *Comput. Methods Biomech. Biomed. Eng.*, vol. 15, no. 2, pp. 131–140, Feb. 2012.

[8] I. Roloff, V. R. Schöffl, L. Vigouroux, and F. Quaine, "Biomechanical model for the determination of the forces acting on the finger pulley system," *J. Biomech.*, vol. 39, no. 5, pp. 915–923, Jan. 2006.

[9] P. Bartolo and B. Bidanda, *Bio-Materials and Prototyping Applications in Medicine*. Berlin, Germany: Springer, 2008.

[10] R. Balasubramanian and V. J. Santos, *The Human Hand as an Inspiration for Robot Hand Development*. Berlin, Germany: Springer, 2014.

[11] J. S. Martell and G. Gini, "Robotic hands: Design review and proposal of new design process," *World Academy Sci., Eng. Technol.*, vol. 26, no. 5, pp. 85–90, 2007.

[12] Z. Xu and E. Todorov, "Design of a highly biomimetic anthropomorphic robotic hand towards artificial limb regeneration," in *Proc. IEEE Int. Conf. Robot. Autom. (ICRA)*, May 2016, pp. 3485–3492.

[13] J. A. E. Hughes, P. Maiolino, and F. Iida, "An anthropomorphic soft skeleton hand exploiting conditional models for piano playing," *Sci. Robot.*, vol. 3, no. 25, Dec. 2018, Art. no. eaau3098.

[14] Y. Zhang, H. Deng, and G. Zhong, "Humanoid design of mechanical fingers using a motion coupling and shape-adaptive linkage mechanism," *J. Bionic Eng.*, vol. 15, no. 1, pp. 94–105, Jan. 2018.

[15] D. Burke, S. C. Gandevia, and G. Macefield, "Responses to passive movement of receptors in joint, skin and muscle of the human hand," *J. Physiol.*, vol. 402, no. 1, pp. 347–361, 1988.

[16] A. B. Swanson, "Flexible implant arthroplasty for arthritic finger joints: Rationale, technique, and results of treatment," *J. Bone Joint Surgery*, vol. 54, no. 3, pp. 435–544, Apr. 1972.

[17] D. E. Foliart, "Swanson silicone finger joint implants: A review of the literature regarding long-term complications," *J. Hand Surgery*, vol. 20, no. 3, pp. 445–449, May 1995.

[18] P. Slade, A. Akhtar, M. Nguyen, and T. Bretl, "Tact: Design and performance of an open-source, affordable, myoelectric prosthetic hand," in *Proc. IEEE Int. Conf. Robot. Autom. (ICRA)*, May 2015, pp. 6451–6456.

[19] F. Rothling, R. Haschke, J. J. Steil, and H. Ritter, "Platform portable anthropomorphic grasping with the bielefeld 20-DOF shadow and 9-DOF TUM hand," in *Proc. IEEE/RSJ Int. Conf. Intell. Robots Syst.*, Oct. 2007, pp. 2951–2956.

[20] C. Melchiorri, G. Palli, G. Berselli, and G. Vassura, "Development of the UB hand IV: Overview of design solutions and enabling technologies," *IEEE Robot. Autom. Mag.*, vol. 20, no. 3, pp. 72–81, Sep. 2013.

[21] D. Chakarov, M. Tsveov, I. Veneva, and P. Mitrouchev, "Adjustable compliance joint with torsion spring for human centred robots," *Int. J. Adv. Robotic Syst.*, vol. 12, no. 12, p. 180, 2015.

[22] H. Yang et al., "A low-cost linkage-spring-tendon-integrated compliant anthropomorphic robotic hand: MCR-Hand III," *Mechanism Mach. Theory*, vol. 158, Apr. 2021, Art. no. 104210.

[23] G. P. Kontoudis, M. Liarokapis, K. G. Vamvoudakis, and T. Furukawa, "An adaptive actuation mechanism for anthropomorphic robot hands," *Frontiers Robot. AI*, vol. 6, p. 47, Jul. 2019.

[24] T. E. Wiste, S. A. Dalley, H. A. Varol, and M. Goldfarb, "Design of a multigrasp transradial prosthesis," *J. Med. Devices*, vol. 5, no. 3, pp. 1–7, Sep. 2011.

[25] G. P. Kontoudis, M. Liarokapis, and K. G. Vamvoudakis, "A compliant, underactuated finger for anthropomorphic hands," in *Proc. IEEE 16th Int. Conf. Rehabil. Robot. (ICORR)*, Jun. 2019, pp. 682–688.

[26] B. Faudot, J.-L. Milan, B. Goislard de Monsabert, T. Le Corroller, and L. Vigouroux, "Estimation of joint contact pressure in the index finger using a hybrid finite element musculoskeletal approach," *Comput. Methods Biomech. Biomed. Eng.*, vol. 23, no. 15, pp. 1225–1235, Nov. 2020.

[27] D. Hu, D. Howard, and L. Ren, "Biomechanical analysis of the human finger extensor mechanism during isometric pressing," *PLoS ONE*, vol. 9, no. 4, Apr. 2014, Art. no. e94533.

[28] K. D. Butz, G. Merrell, and E. A. Nauman, "A three-dimensional finite element analysis of finger joint stresses in the MCP joint while performing common tasks," *HAND*, vol. 7, no. 3, pp. 341–345, Sep. 2012.

[29] H. I. Relf, C. G. Barberio, and D. M. Espino, "A finite element model for trigger finger," *Prosthesis*, vol. 2, no. 3, pp. 168–184, Jul. 2020.

[30] Y. Wei, Z. Zou, G. Wei, L. Ren, and Z. Qian, "Subject-specific finite element modelling of the human hand complex: Muscle-driven simulations and experimental validation," *Ann. Biomed. Eng.*, vol. 48, no. 4, pp. 1181–1195, 2019.

[31] G. Harih, R. Nohara, and M. Tada, "Finite element digital human hand model-case study of grasping a cylindrical handle," *J. Ergonom.*, vol. 7, no. 2, 2017, doi: 10.4172/2165-7556.1000190.

[32] C. J. De Luca, L. D. Gilmore, M. Kuznetsov, and S. H. Roy, "Filtering the surface EMG signal: Movement artifact and baseline noise contamination," *J. Biomech.*, vol. 43, no. 8, pp. 1573–1579, May 2010, doi: 10.1016/j.jbiomech.2010.01.027.

[33] F. D. Farfán, J. C. Politti, and C. J. Felice, "Evaluation of EMG processing techniques using information theory," *Biomed. Eng. OnLine*, vol. 9, no. 1, p. 72, Dec. 2010, doi: 10.1186/1475-925X-9-72.

[34] F. H. Netter, *Atlas of Human Anatomy E-Book*. Amsterdam, The Netherlands: Elsevier, 2017.

[35] S. Z. Glickel and O. A. Barron, "Proximal interphalangeal joint fracture dislocations," *Hand Clinics*, vol. 16, no. 3, pp. 333–344, Aug. 2000.

[36] S. D. Carrigan, R. A. Whiteside, D. R. Pichora, and C. F. Small, "Development of a three-dimensional finite element model for carpal load transmission in a static neutral posture," *Ann. Biomed. Eng.*, vol. 31, no. 6, pp. 718–725, Jun. 2003.

[37] C. C.-D. La Portilla, C. Pasapula, R. Larrainzar-Garijo, and J. Bayod, "Finite element analysis of secondary effect of midfoot fusions on the spring ligament in the management of adult acquired flatfoot," *Clin. Biomech.*, vol. 76, Jun. 2020, Art. no. 105018.

[38] M. Adouni and A. Shirazi-Adl, "Partitioning of knee joint internal forces in gait is dictated by the knee adduction angle and not by the knee adduction moment," *J. Biomech.*, vol. 47, no. 7, pp. 1696–1703, May 2014.

[39] P. Tanska, M. E. Mononen, and R. K. Korhonen, "A multi-scale finite element model for investigation of chondrocyte mechanics in normal and medial meniscectomy human knee joint during walking," *J. Biomech.*, vol. 48, no. 8, pp. 1397–1406, Jun. 2015.

[40] G.-T. Lin, W. P. Cooney, P. C. Amadio, and K.-N. An, "Mechanical properties of human pulleys," *J. Hand Surgery*, vol. 15, no. 4, pp. 429–434, Aug. 1990.

[41] D. Chamoret, M. Bodo, and S. Roth, "A first step in finite-element simulation of a grasping task," *Comput. Assist. Surgery*, vol. 21, pp. 22–29, Dec. 2016, doi: 10.1080/24699322.2016.1240294.

[42] L. Zollo, S. Roccella, E. Guglielmelli, M. C. Carrozza, and P. Dario, "Biomechatronic design and control of an anthropomorphic artificial hand for prosthetic and robotic applications," *IEEE/ASME Trans. Mechatronics*, vol. 12, no. 4, pp. 418–429, Aug. 2007.

[43] M. A. Roa and R. Suárez, "Grasp quality measures: Review and performance," *Auto. Robots*, vol. 38, no. 1, pp. 65–88, 2015.

[44] B. Leon, J. L. Sancho-Bru, N. J. Jarque-Bou, A. Morales, and M. A. Roa, "Evaluation of human prehension using grasp quality measures," *Int. J. Adv. Robotic Syst.*, vol. 9, no. 4, p. 112, 2012.

[45] C. Rubert, B. León, A. Morales, and J. Sancho-Bru, "Characterisation of grasp quality metrics," *J. Intell. Robotic Syst.*, vol. 89, nos. 3–4, pp. 319–342, Mar. 2018.

[46] Y. Wei, Z. Zou, Z. Qian, L. Ren, and G. Wei, "Biomechanical analysis of the effect of the finger extensor mechanism on hand grasping performance," *IEEE Trans. Neural Syst. Rehabil. Eng.*, vol. 30, pp. 360–368, 2022.

[47] M. Ciocarlie, A. Miller, and P. Allen, "Grasp analysis using deformable fingers," in *Proc. IEEE/RSJ Int. Conf. Intell. Robots Syst.*, Aug. 2005, pp. 4122–4128.

[48] C. Noel, "A three-dimensional visco-hyperelastic FE model for simulating the mechanical dynamic response of preloaded phalanges," *Med. Eng. Phys.*, vol. 61, pp. 41–50, Nov. 2018.

[49] Q. Bi, C.-J. Yang, X.-L. Deng, and J.-C. Fan, "Human finger mechanical impedance modeling: Using multiplicative uncertain model," *Proc. Inst. Mech. Eng., C, J. Mech. Eng. Sci.*, vol. 230, no. 12, pp. 1978–1986, Jul. 2016.

[50] J. Z. Wu, R. G. Dong, T. W. McDowell, and D. E. Welcome, "Modeling the finger joint moments in a hand at the maximal isometric grip: The effects of friction," *Med. Eng. Phys.*, vol. 31, no. 10, pp. 1214–1218, Dec. 2009.

[51] D. L. Jindrich, A. D. Balakrishnan, and J. T. Dennerlein, "Finger joint impedance during tapping on a computer keyswitch," *J. Biomech.*, vol. 37, no. 10, pp. 1589–1596, Oct. 2004.

[52] D. G. Kamper, T. G. Hornby, and W. Z. Rymer, "Extrinsic flexor muscles generate concurrent flexion of all three finger joints," *J. Biomech.*, vol. 35, no. 12, pp. 1581–1589, Dec. 2002.

[53] P.-H. Kuo and A. D. Deshpande, "Muscle-tendon units provide limited contributions to the passive stiffness of the index finger metacarpophalangeal joint," *J. Biomech.*, vol. 45, no. 15, pp. 2531–2538, Oct. 2012.

[54] W. N. Timm, S. W. O'Driscoll, M. E. Johnson, and K.-N. An, "Functional comparison of pronation and supination strengths," *J. Hand Therapy*, vol. 6, no. 3, pp. 190–193, Jul. 1993.

[55] W. Zhang, V. M. Zatsiorsky, and M. L. Latash, "Finger synergies during multi-finger cyclic production of moment of force," *Exp. Brain Res.*, vol. 177, no. 2, pp. 243–254, Feb. 2007.